AIAA JOURNAL
Vol. 39, No. 8, August 2001

System Identification and Proper Orthogonal Decomposition Method Applied to Unsteady Aerodynamics

Deman Tang* and Denis Kholodar†
Duke University, Durham, North Carolina 27708-0300
Jer-Nan Juang‡
NASA Langley Research Center, Hampton, Virginia 23681-0001
and
Earl H. Dowell§
Duke University, Durham, North Carolina 27708-0300

The representation of unsteady aerodynamic flowfields in terms of global aerodynamic modes has proven to be a useful method for reducing the size of the aerodynamic model over those representations that use local variables at discrete grid points in the flow field. Eigenmodes and proper orthogonal decomposition modes have been used for this purpose with good effect. This suggests that system identification models may also be used to represent the aerodynamic flowfield. Implicit in the use of a systems identification technique is the notion that a relative small state-space model can be useful in describing a dynamical system. The proper orthogonal decomposition model is first used to show that indeed a reduced-order model can be obtained from a much larger numerical aerodynamical model (the vortex lattice method is used for illustrative purposes), and the results from the proper orthogonal decomposition model and the system identification methods are then compared. For the example considered the two methods are shown to give comparable results in terms of accuracy and reduced model size. The advantages and limitations of each approach are briefly discussed. Both appear promising and complementary in their characteristics.

Nomenclature

a	=	generalized coordinate in proper orthogonal decomposition method
c	=	delta-wing root chord
H	=	Hankel matrix
km, kn	=	numbers of vortex elements on delta wing
kmm	=	total number of vortices on both the delta wing and wake in the x direction
L	=	total lift
l	=	delta-wing span
$\hat{Q}$	=	flow variable matrix
$q(j)$	=	flow variable at spatial point and at time j
t	=	time
U	=	airspeed
w	=	downwash
x, y	=	streamwise and spanwise coordinates
Γ	=	vortex strength
Δp	=	aerodynamic pressure loading on panel
$\overline{\Delta p}$	=	nondimensional aerodynamic pressure, $\Delta p/(\rho_\infty U^2)$
Δt	=	time step
Δx	=	plate element length in the streamwise direction
Δy	=	plate element length in the spanwise direction
Λ	=	diagonal matrix of eigenvalue, λ
λ_i	=	continuous time eigenvalues, $\lambda_i = \mathrm{Log}(\Lambda)/\Delta t$
ρ_∞	=	air density
Σ	=	diagonal matrix of singular values, σ
σ	=	singular values of $\hat{Q}$
τ	=	nondimensional time
Ψ	=	matrix of eigenvectors corresponding to eigenvalue matrix, Λ
ψ_i	=	eigenvectors corresponding to eigenvalues, λ_i

Received 15 September 2000; revision received 27 January 2001; accepted for publication 29 January 2001.

*Research Associate Professor, Department of Mechanical Engineering and Materials Science. Member AIAA.
†Research Assistant, Department of Mechanical Engineering and Materials Science. Member AIAA.
‡Principal Scientist, Structural Dynamics Branch. Fellow AIAA.
§J. A. Jones Professor, Department of Mechanical Engineering and Materials Science. Fellow AIAA.

Introduction

In recent work it has been shown that the use of a modal representation of unsteady aerodynamic flowfields has many advantages.[1–4] Among these is the ability to reduce the order of a computational fluid dynamics (CFD) code from many thousands of degrees of freedom to several tens of degrees of freedom while retaining essentially the same accuracy of representation of fluid forces acting on a wing. Recognizing that the aerodynamic forces can be expressed in terms of aerodynamic modes, this suggests that in some cases it may be advantageous to use a system identification method to determine a modal representation of the aerodynamic forces. For example, this could be done using either numerical data from a CFD code or experimental data from a wind-tunnel test. Here we explore this possibility and compare the results obtained from a system identification procedure and those obtained by a direct determination of the aerodynamic modes from a theoretical fluid dynamics model. In the present study a three-dimensional time domain vortex lattice aerodynamic model and the proper orthogonal decomposition (POD) method are used to investigate the unsteady flow about an oscillating delta wing. The POD modes and the eigenmodes of the vortex lattice model are determined starting from a time history of the flowfield computed for a step change in angle of attack (or plunge velocity). This same set of time histories is then provided as the input data for a system identification technique as discussed in Ref. 5 to determine a dynamic model of the aerodynamic system. The eigenvalues of this identified system are then compared to those determined using the POD method and the vortex lattice model. Excellent agreement is found between the two results, thus confirming the ability of system identification methods to extract useful information from numerically determined time histories based upon a theoretical computational model. This also suggests that a similar procedure that employs numerical data from more complex CFD models or from measured experimental data might be successful. In the following sections, discussed in order are the aerodynamic model, the POD method, the system identification

method, and an example using numerical data from a simulated time history.

Aerodynamic Model

The flow about a cantilevered half-span delta wing is assumed to be incompressible, inviscid, and irrotational. Here an unsteady vortex lattice method is used to model this flow. Kim[4] has also used a similar flow model in his study of the POD or Karhunen–Loeve method for a wing of rectangular planform. A typical planar vortex lattice mesh for the three-dimensional flow over a delta wing is shown in Fig. 1. The plate and wake are divided into a number of elements. In the wake and on the wing all of the elements are of equal size Δx in the streamwise direction. For the present calculations the spanwise element size Δy is chosen to be equal to Δx. Point vortices are placed on the plate and in the wake at the quarter chord of the elements. At the three-quarter chord of each plate element, a collocation point is placed for the downwash; the velocity induced by the discrete vortices is set equal to the downwash arising from the step angle of attack of the delta wing. Thus one has the relationship

$$w_i^{t+1} = \sum_{j}^{kmm} K_{ij}\Gamma_j^{t+1}, \qquad i = 1, \ldots, km \tag{1'}$$

where w_i^{t+1} is the downwash at the ith collocation point at time step $t+1$, Γ_j is the strength of the jth vortex. Γ is normalized by cU and w by U, where U is the freestream velocity. K_{ij} is an aerodynamic kernel function. (A separate equation numbering system is used in this section as distinct from that employed in the remainder of the paper. This is to distinguish between the aerodynamic model per se and the system identification methodology.) An aerodynamic matrix equation to determine Γ can be expressed as

$$[A]\{\Gamma\}^{t+1} + [B]\{\Gamma\}^{t} = [T]\{w\}^{t+1} \tag{2'}$$

where $[A]$ and $[B]$ are aerodynamic coefficient matrices and $[T]$ is a transfer matrix for determining the relationship between the global vortex lattice mesh and the local vortex lattice mesh on the delta wing itself. Expressions for A, B, and T are given in Ref. 1.

From the fundamental aerodynamic theory the pressure distribution on the wing can be obtained at the jth point in terms of the vortex strengths. The pressure difference between the wing plate upper and lower surfaces at $x = x_j$, $y = y_j$ is given by

$$\Delta p^{t+1}(x_j, y_j) = \rho U^2 \frac{c}{\Delta x}\left\{(\Gamma^{t+1}(x_j, y_j) + \sum_{i=1}^{j}\left[\Gamma^{t+1}(x_i, y_j) - \Gamma^{t}(x_i, y_j)\right]\right\} \tag{3'}$$

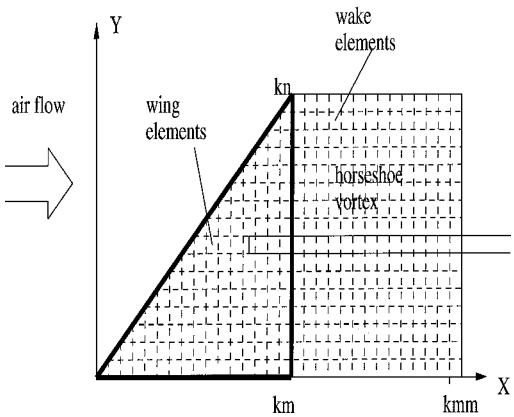

Fig. 1 Numerical grid for a delta-wing plate using a vortex lattice aerodynamic model.

The local total lift at $y = y_j$ is obtained by integrating the pressure difference along the local chord line:

$$L_{\text{local}}^{t+1}(y_j) = \int_0^{c_{\text{local}}} \Delta p^{t+1}(x, y_j)\,\mathrm{d}x$$

where $c_{\text{local}} = cy_j/l$, l is span length, and c is the root chord.

The total lift is obtained by integrating the local total lift along the span:

$$L^{t+1} = \int_0^{l} L_{\text{local}}^{t+1}(y)\,\mathrm{d}y = c\sum_{j=1}^{k_n} L_{\text{local}}^{t+1}(y_j)\Delta\bar{y}$$

where $\Delta\bar{y} = 1/k_n$ and k_n is the number of spanwise discrete elements.

The total aerodynamic lift coefficient C_L is defined by

$$C_L^{t+1} = L^{t+1}\Big/\tfrac{1}{2}\rho U^2 A_w \tag{4'}$$

where A_w is the total wing area. In the present example $A_w = \frac{1}{2}c^2$ and $\Delta\bar{y} = \frac{1}{15}$.

The numerical model is a simple delta-wing configuration with a leading-edge sweep of 45 deg. We use an aerodynamic vortex lattice model with 120 vortex elements on the delta wing ($km = kn = 15$) and 525 vortex elements in the wake ($kmm = 50$). The total number of vortex elements is $N = 645$.

Singular Value Decomposition, Proper Orthogonal Decomposition and Balanced Modes: A Generic Discussion

Let $q(j)$ be the nth flow variable at some spatial point at some time j where $n = 1, \ldots, N$ and $j = 1, \ldots, J$. Now form the matrix $\hat{Q}$ as

$$[\hat{Q}]_{N\times J} = \begin{bmatrix} q^1(1) & \ldots & q^1(J) \\ \vdots & \vdots & \vdots \\ q^N(1) & \ldots & q^N(J) \end{bmatrix} \tag{1}$$

Again note the total number of time steps is J, and the total number of flow variables is N. For a typical CFD calculation J might be 1000 and N might be 10,000 or more. Hence N is much greater than J.

Now assume a singular value decomposition of $\hat{Q}$, i.e.,

$$[\hat{Q}] = [U][\Sigma][V]^T \tag{2}$$

where U is a unitary matrix of dimension $N \times n$ and V is also a unitary matrix of dimension $J \times n$. One may select n and typically n will be less than J. Note that

$$[U]^T[U] = [I]_{n\times n}, \qquad [V]^T[V] = [I]_{n\times n} \tag{3}$$

i.e.,

$$[\Sigma]_{n\times n} = \begin{bmatrix} \sigma_1 & & & \\ & \sigma_2 & & \\ & & \ddots & \\ & & & \sigma_n \end{bmatrix} \tag{4}$$

Now order these singular values such that

$$\sigma_1 \geq \sigma_2 \geq \cdots \sigma_n \tag{5}$$

Now form Φ, the correlation matrix for the POD method:

$$[\Phi] \equiv [\hat{Q}]^T[\hat{Q}] = [V][\Sigma]^T[U]^T[U][\Sigma][V]^T = [V][\Sigma]^T[\Sigma][V]^T \tag{6}$$

Equation (6) implies that V is the eigenvector of the correlation matrix and the corresponding eigenvalues are the squares of the singular values.

From Eq. (2), one can compute (assuming that V is normalized so that the magnitude of each eigenvector is unity)

$$[\hat{Q}][V] = [U][\Sigma][V]^T[V] = [U][\Sigma] \tag{7}$$

One can also compute U from Eq. (7), and further one can compute $\hat{Q}$ from a knowledge of U, V and the singular values using Eq. (2). Usually it is easier to compute $\hat{Q}$ directly from Eq. (1). However the representation of Eq. (2) can be useful if one chooses to decompose $\hat{Q}$ such that

$$[\hat{Q}] = \left([U][\Sigma]^{\frac{1}{2}}\right)\left([\Sigma]^{\frac{1}{2}}[V]^T\right) \tag{8}$$

With this decomposition the POD modes are said to be "balanced," and these are often put forth as an optimum choice for mode selection.

If there is a truncation in the singular values, i.e., one chooses n to be less than J, which is much less than N, then Eq. (2) can be written in a reduced form. The corresponding reduced form for $\hat{Q}$ approaches the original $\hat{Q}$ if the neglected singular values or POD eigenvalues are sufficiently small compared to those retained.

Denoting V as the eigenvector matrix for the correlation matrix of dimension $J \times n$, noting that $\hat{Q}$ is a matrix of $N \times J$, and defining a as the new unknowns to be determined, which are the n modal amplitudes of the POD modes, then one can write the original flow variables q as

$$\left\{q^{(t)}\right\}_{N\times 1} = [\hat{Q}]_{N\times J}[V]_{J\times n}\{a\}_{n\times 1} \tag{9}$$

Substituting this expression into a generic form of the flow equations of motion, i.e.,

$$\left\{\frac{\mathrm{d}q}{\mathrm{d}t}\right\} = \{Q(q)\} + \{B\}u \tag{10}$$

and premultiplying by the transpose of $\hat{Q}$ gives a reduced-order model in terms of the new unknowns a, where the dimension of the vector a is $n \times 1$ with n chosen to be less than J.

For simplicity, in Eq. (10) only a single scalar input u is shown. The generalization to multiple inputs is clear. If $Q(q)$ in Eq. (10) is expanded in a Taylor series about a steady flow solution (the time linearized model corresponds to retaining only linear terms in q in the Taylor series), then a particularly simple and attractive form of the reduced-order model is obtained.

There is another interesting case to consider, which may arise when experimental data rather than numerical data from a CFD code are used to construct a reduced-order model. In this case the number of flow variables that are observed or measured N will be relatively small and typically N will be less than J, the total number of time steps for which data are obtained. Formally the calculation still goes through, but now the number of flow variables modeled is much smaller than for a CFD code. Ideally these flow variables would be related to the amplitudes of the dominant modes of the flow. Some preliminary results for this case are included in the numerical examples discussed later.

System Identification

To conform to the usual formalism of system identification theory, we consider a discrete time state-space model.[4] The vortex lattice flow model naturally appears in this form. For continuous time models the relationship between discrete and continuous time representations must be carefully considered. Formally the procedure is similar, however.

Assume that the flowfield can be described by the discrete-time state-space model

$$x(k+1) = Ax(k) + Bu(k), \qquad y(k) = Cx(k) + Du(k) \tag{11}$$

where $x(k)$ is a state vector of $n \times 1$ ($n =$ order of the system), $u(k)$ is an input force vector of $\gamma \times 1$ ($\gamma =$ number of input), $y(k)$ is an output measurement vector of $m \times 1$ ($m =$ number of output). The matrices A, B, C, and D are the state matrix, input matrix, output matrix, and direct transmission matrix, respectively.

Let $u_i(0) = 1$ $(i = 1, 2, \ldots, \gamma)$ and $u_i(k) = 0$ $(k = 1, 2, \ldots,)$ be substituted into Eq. (11). When the substitution is performed for each input element $u_i(0) = 1$ $(i = 1, 2, \ldots, \gamma)$, the results can be assembled into a pulse response matrix Y with dimension m by r as follows:

$$Y_0 = D, \qquad Y_1 = CB, \qquad Y_2 = CAB, \ldots, \qquad Y_k = CA^{k-1}B \tag{12}$$

The constant matrices in the sequence are known as Markov parameters.[4]

Assume that the scalar quantity $q_i(k)$ in the matrix Q in Eq. (1) is the pulse response of the ith flow variable at the time step k corresponding to a pulse input. A column vector Y can be formed by

$$Y_1 = CB = \begin{bmatrix} q_1(1) \\ q_2(1) \\ \vdots \\ \vdots \\ q_m(1) \end{bmatrix}, \qquad Y_2 = CAB = \begin{bmatrix} q_1(2) \\ q_2(2) \\ \vdots \\ \vdots \\ q_m(2) \end{bmatrix}$$

$$\ldots Y_k = CA^{k-1}B = \begin{bmatrix} q_1(k) \\ q_2(k) \\ \vdots \\ \vdots \\ q_m(k) \end{bmatrix} \tag{13}$$

System identification begins by forming the generalized Hankel matrix $H(0)$, composed of the Markov parameters:

$$H(0) = [Y_1 \quad Y_2 \quad \cdots \quad Y_{l-1}] \tag{14}$$

This matrix is identical to the matrix Q in Eq. (1) with the absence of the last column. Here an assumption has been made, i.e., $m > l > n$. For the other cases where the number of measurement sensors is sufficiently less than the order of the system, i.e., $l > n > m$, a different Hankel matrix can be formed for system identification.[5] The fundamental rule is that the Hankel matrix must be formed such that its rank is larger than the order of the system to be identified.

In theory, the Hankel matrix $H(0)$ and the state-space model are related by

$$\begin{aligned} H(0) &= [Y_1 \quad Y_2 \quad \cdots \quad Y_{l-1}] \\ &= [CB \quad CAB \quad \cdots \quad CA^{l-2}B] \\ &= C[B \quad AB \quad \cdots \quad A^{l-2}B] \end{aligned} \tag{15}$$

To determine A, B, C, first decompose the matrix $H(0)$ by using singular value decomposition to yield

$$\begin{aligned} H(0) &= U\Sigma V^T = [U_r U_t]\begin{bmatrix} \Sigma_r & O_{n-r} \\ O_{n-r} & \Sigma_t \end{bmatrix}[V_r V_t]^T \\ &= U_r \Sigma_r V_r^T + U_t \Sigma_t V_t^T \\ &\approx U_r \Sigma_r V_r^T \\ &= \left[U_r \Sigma_r^{\frac{1}{2}}\right]\left[\Sigma_r^{\frac{1}{2}} V_r\right] \end{aligned} \tag{16}$$

Comparison of Eqs. (15) and (16) establishes the following equalities:

$$\left[U_r \Sigma_r^{\frac{1}{2}}\right] = C, \qquad \left[\Sigma_r^{\frac{1}{2}} V_r\right] = [B \quad A \quad \cdots \quad A^{l-2}] \tag{17}$$

The equalities are not unique, but they are balanced because both share the matrix Σ equally. The matrix B is then determined by

$$B = \text{the first column of } \left[\Sigma_r^{\frac{1}{2}} V_r\right] \tag{18}$$

To determine the state matrix A, another Hankel matrix must be formed, i.e.,

$$H(1) = [Y_2 \quad Y_3 \quad \cdots \quad Y_l] \tag{19}$$

This matrix is formed by deleting the first column of $H(0)$ and adding a new column at the end of the matrix. As a result, $H(1)$ has the following relationship with the system matrices A, B, and C:

$$\begin{aligned} H(1) &= [Y_2 \quad Y_3 \quad \cdots \quad Y_l] \\ &= [CAB \quad CA^2B \quad \cdots \quad CA^{l-1}B] \\ &= CA[B \quad AB \quad \cdots \quad A^{l-2}B] \end{aligned} \tag{20}$$

Substituting Eq. (17) into Eq. (20) thus yields

$$\begin{aligned} A &= \left[U_r \Sigma_r^{-\frac{1}{2}}\right]^{\dagger} H(1) \left[\Sigma_r^{-\frac{1}{2}} V_r\right]^{\dagger} \\ &= \Sigma_r^{-\frac{1}{2}} U_r^T H(1) V_r^T \Sigma_r^{-\frac{1}{2}} \end{aligned} \tag{21}$$

The symbol † means pseudo-inverse. The orthonormal property of U and V shown in Eq. (3) has been used to derive Eq. (21).

Assume that the state matrix A of order r has a complete set of linearly independent eigenvectors $\psi_1, \psi_2, \ldots, \psi_r$ with corresponding eigenvalues $\lambda_1, \lambda_2, \ldots, \lambda_r$, which are not necessarily distinct. Define Λ as the diagonal matrix of eigenvalues and Ψ as the matrix of eigenvectors, i.e.,

$$\Lambda = \begin{bmatrix} \lambda_1 & & & & \\ & \lambda_2 & & & \\ & & \cdot & & \\ & & & \cdot & \\ & & & & \lambda_r \end{bmatrix} \tag{22}$$

$$\Psi = [\psi_1 \quad \psi_2 \quad \cdots \quad \psi_r] \tag{23}$$

The identified A, B, and C can then be transformed to become Λ, $\Psi^{-1}B$, and $C\Psi$. The diagonal matrix Λ contains the information of modal damping rates and damped natural frequencies. The matrix $\Psi^{-1}B$ defines the initial modal amplitudes and the matrix $C\Psi$ the mode shape at the sensor points. All of the modal parameters of a dynamic system can thus be identified by the three matrices Λ, $\Psi^{-1}B$, and $C\Psi$. The desired modal damping rates and damped natural frequencies are simply the real and imaginary parts of the eigenvalues Λ_c, after transformation from the discrete-time domain to the continuous-time domain using the relationship

$$\Lambda_c = (1/\Delta t)\,\mathrm{Log}(\Lambda) \tag{24}$$

Example

POD Model

In this example $J = 100$ time steps, and Eq. (2′) is marched in time to determine Γ for a unit step change in angle of attack. Identifying Γ with the flow variables q, we form $\hat{Q}$ and Φ [see Eqs. (1) and (6)]. From Eq. (6) one obtains the POD eigenvector V and the corresponding POD eigenvalues of $\Sigma^T\Sigma$. We normalize the POD eigenvectors V such that

$$[V]^T[V] = [I]$$

The POD eigenvalues calculated are shown in Table 1. Examining these 100 eigenvalues, one finds the first few modes are the most important. Also found are some very small negative eigenvalues because of the numerical roundoff error in the eigenvalue calculation. Note that the POD eigenvalues and eigenvectors are *not* the eigenvalues and eigenvectors of Γ per se. The latter maybe determined from Eq. (2′) or approximately from the reduced-order model.

From Eq. (2) we can determine the unitary matrix U

$$[U] = [\hat{Q}][V][\Sigma]^{-1} \tag{25}$$

with a normalization such that $[U]^T[U] = [I]$

From Eq. (2′) we have

$$\{\Gamma\}^{t+1} + [A]^{-1}[B]\{\Gamma\}^t = [A]^{-1}[T]\{w\}^{t+1} \tag{26}$$

Table 1 Eigenvalues σ_n

σ_{1-25}	σ_{26-50}	σ_{51-75}	σ_{76-100}
0.31168E+03	0.51654E+00	0.82697E−05	−0.33688E−05
0.33737E+02	0.50582E+00	−0.80430E−05	−0.30680E−05
0.39184E+01	0.49650E+00	−0.77611E−05	−0.26678E−05
0.31482E+01	0.48854E+00	−0.72553E−05	−0.27129E−05
0.25025E+01	0.48179E+00	0.75330E−05	−0.22659E−05
0.20812E+01	0.47621E+00	0.72555E−05	−0.16534E−05
0.17607E+01	0.47171E+00	−0.69035E−05	0.32531E−05
0.15281E+01	0.46827E+00	−0.65890E−05	0.29655E−05
0.13464E+01	0.46584E+00	−0.62088E−05	0.28340E−05
0.12051E+01	0.46439E+00	−0.64251E−05	0.25623E−05
0.10909E+01	0.15028E+00	−0.57141E−05	0.24380E−05
0.99799E+00	0.85771E−02	0.65583E−05	−0.13306E−05
0.92088E+00	0.84648E−04	0.64960E−05	−0.11599E−05
0.85612E+00	−0.17071E−04	0.60496E−05	−0.84823E−05
0.80130E+00	0.13413E−04	0.57069E−05	−0.46961E−05
0.75427E+00	0.12234E−04	−0.52226E−05	−0.34102E−06
0.71385E+00	−0.10651E−04	−0.48201E−05	−0.12280E−06
0.67867E+00	−0.10369E−04	−0.42629E−05	0.18361E−05
0.64813E+00	0.11271E−04	0.49989E−05	0.17704E−05
0.62129E+00	0.10661E−04	0.47778E−05	0.14315E−05
0.59783E+00	−0.90705E−05	0.47381E−05	0.12146E−05
0.57712E+00	0.99622E−05	0.43455E−05	0.10583E−05
0.55896E+00	0.96568E−05	0.39997E−05	0.44381E−06
0.54293E+00	0.90764E−05	−0.37350E−05	0.49844E−06
0.52889E+00	−0.85099E−05	−0.35918E−05	0.60061E−06

From Eq. (9) we have

$$\{\Gamma\} = [\hat{Q}]_{N\times J}[V]_{J\times n}\{a\}_n$$

Substituting Eq. (25) into Eq. (9), we have

$$\{\Gamma\} = [U][\Sigma]\{a\} \tag{27}$$

Substituting Eq. (27) into Eq. (26), we have

$$[U][\Sigma]\{a\}^{t+1} + [A]^{-1}[B][U][\Sigma]\{a\}^t = [A]^{-1}[T]\{w\}^{t+1} \tag{28}$$

Premultiplying by the transpose of $[U][\Sigma]$ gives a reduced-order model in terms of the new unknowns $\{a\}$:

$$\begin{aligned} &([U][\Sigma])^T[U][\Sigma]\{a\}^{t+1} + ([U][\Sigma])^T[A]^{-1}[B][U][\Sigma]\{a\}^t \\ &\quad = ([U][\Sigma])^T[A]^{-1}[T]\{w\}^{t+1} \end{aligned} \tag{29}$$

Thus a new three-dimensional time domain vortex lattice aerodynamic equation is given by

$$\{a\}^{t+1}_{n\times 1} + [P]_{n\times n}\{a\}^t_{n\times 1} = [R]_{n\times N}\{w\}^{t+1}_{N\times 1} \tag{30}$$

where

$$[P] = ([\Sigma]^T[\Sigma])^{-1}([U][\Sigma])^T[A]^{-1}[B][U][\Sigma]$$

$$[R] = ([\Sigma]^T[\Sigma])^{-1}([U][\Sigma])^T[A]^{-1}[T]$$

Generally, $n \ll N$, and thus a reduced-order time domain equation is obtained. For the present example $N = 645$ and $n \leq 20$.

Once $\{a\}$ is determined from Eq. (30), the $\{\Gamma\}^t$ and $\{\Gamma\}^{t+1}$ can be determined from Eq. (26), and the total lift coefficient of the delta wing is calculated using Eq. (4′).

Figure 2 shows the total lift coefficient of the delta wing vs nondimensional time τ as determined from the full vortex lattice model, i.e., using Eq. (2′) with $N = 645$.

Figure 3 shows the total lift coefficient of the delta wing vs nondimensional time τ as determined from the reduced-order model for various sizes of the reduced-order model, i.e., $n = 1$, 5 and $n = 20$, using Eq. (30). For larger τ all results are virtually the same.

The reduced-order model results are very close to the result using the full vortex lattice model for the steady state, $\tau \to \infty$ even for $n = 1$. These results are consistent with those of Table 1. As seen

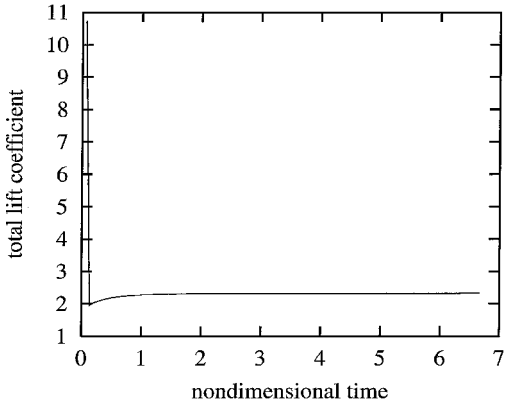

Fig. 2 Total lift coefficient of the delta wing vs nondimensional time τ with all modes retained.

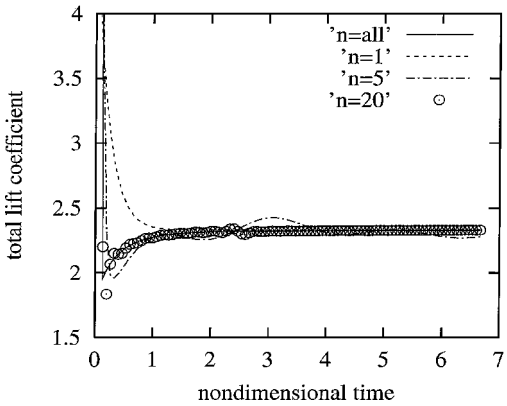

Fig. 3 Total lift coefficient of the delta wing vs nondimensional time τ for $n = 1$, 5 and $n = 20$.

from this table, the POD eigenvalue of the first mode is significantly larger than the others. So there is a single dominant mode, and all others have a relatively smaller contribution to the total lift coefficient. However more POD modes are required to capture the dynamics of the flow model for shorter times, say $\tau < 1$, as shown in Fig. 3.

The aerodynamic eigenvalues of the vortex lattice model can be determined from Eq. (26), and an approximation to these eigenvalues can be determined from Eq. (30) by setting the right-hand sides to zero and determining the condition for nontrivial solutions in the usual way. Results from these calculations will be compared to those obtained from the system identification method in the following discussion.

System Identification

Using the time history for the vortex strengths of the vortex lattice model at each grid point, the system identification procedure described earlier was used to construct a dynamical model of this system. By using all of the information of the original model, we can be sure that we will reproduce these same time histories to some specified accuracy, and that is indeed the case. Within plotting error the results for the time history of the original vortex lattice model and that of the identified model are identical.

More interesting is the number of states required in the system identification model to achieve this accuracy and how well the eigenvalues of the identified model agree with those of the original model. It turns out that the number of states in the identified model is about 40, i.e., of the same order has the number of states required in the POD model to reproduce the essential dynamics of the original vortex lattice model.

It has been shown in previous work that the dominant eigenvalues of the vortex lattice model may be represented by the POD modes. In Fig. 4 we show a comparison between the eigenvalues determined from the full vortex model and those determined from the system identification model. As is seen, the agreement between the two results is excellent for the corresponding eigenvalues. The identified

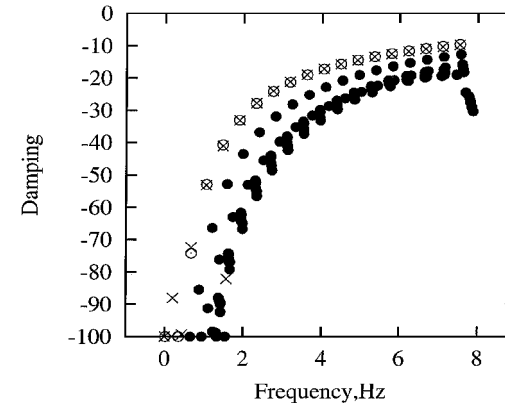

Fig. 4 Eigenvalues of vortex lattice model for unsteady three-dimensional flow about a delta wing. Eigenvalues determined directly from the vortex lattice model: ∘, dominant branch of eigenvalues; ●, all other eigenvalues; and ×, eigenvalues from system identification model.

model in fact has represented the eigenmodes in the dominant branch of the eigenvalue distribution of the original vortex lattice model and done so with a high degree of accuracy.

The dominant branch of the eigenvalue distribution corresponds to the eigenmodes with a spanwise pressure distribution similar to that for the lift on a wing at steady angle of attack. Other branches of the eigenvalue distribution correspond to higher spanwise modal forms.

A system identification (SID) model for an unsteady aerodynamic flow has been created for several wing motions or gust excitations and corresponding aerodynamic responses. These models were derived from numerical simulations using a vortex lattice (VL) model for the delta wing with 55 vortex elements on the wing and 300 vortex elements in the wake (e.g., $km = kn = 10$, $kmm = 40$ as shown in Fig. 1). In each case the flow about the wing is excited by a certain type of prescribed downwash at the wing grid points $w(t)$. The numerical VL model produced vortex strengths at the grid points of the wing and in the wake $\Gamma(t)$ and the corresponding pressure distribution on the wing $p(t)$. These data were then used as input for the SID code.

The excitations to the flow that have been considered are 1) step angle of attack $w(t) = \text{const}$ for $t > 0$; 2) sharp edge gust $w(t - x/u) = \text{const}$ for $(t - x/u) > 0$; and 3) frozen gust of changing frequency $w(t - x/u) = \text{const} \times \sin[\omega(t - x/u)^2/2T]$, which is sometimes called a swept gust; and finally 4) random downwash (w at each grid point and at every time step is a random number).

First, the SID model was used to reproduce the time histories of the vortex strength (on the wing and in the wake) for 100 time steps. Results obtained from the SID model were almost identical to those of the original VL model. The plots of such time histories are not provided here because one would not be able to see the difference in the time series of the original data and the time series obtained via SID, so closly do they agree. However, to quantify the differences between VL and SID outputs, an error δ, defined as $\delta = 100\%|Q - y|/|Q|$, was used, where the norm $|X|$ is defined to be the largest singular value of X. In this case, both Q (VL) and y (SID) are 100×355 rectangular matrices (100 time steps and 355 degrees of freedom). For the just-mentioned aerodynamic problems and given the vortex strengths everywhere, the error was less than 0.05%. Moreover, using the VL time series for the vortex strengths only on the wing, the SID model reproduced them with almost the same accuracy—the largest (among the aforementioned cases) error was 0.1%. The number of singular values retained in the identified model varied from 60 to 90 for the cases when vortex strengths were provided only on the wing and from 60 to 160 for the cases when the SID used vortex strengths both on the wing and in the wake. (The number of singular values kept was such that the ratio of the largest singular value to the smallest one kept was 10^{-12}.)

Next the ability of such a SID model to capture the eigenmodes of the original VL system and especially the dominant eigenmodes was studied. Here again, all of the information on the wing and wake was used initially, and then the information only on the wing was

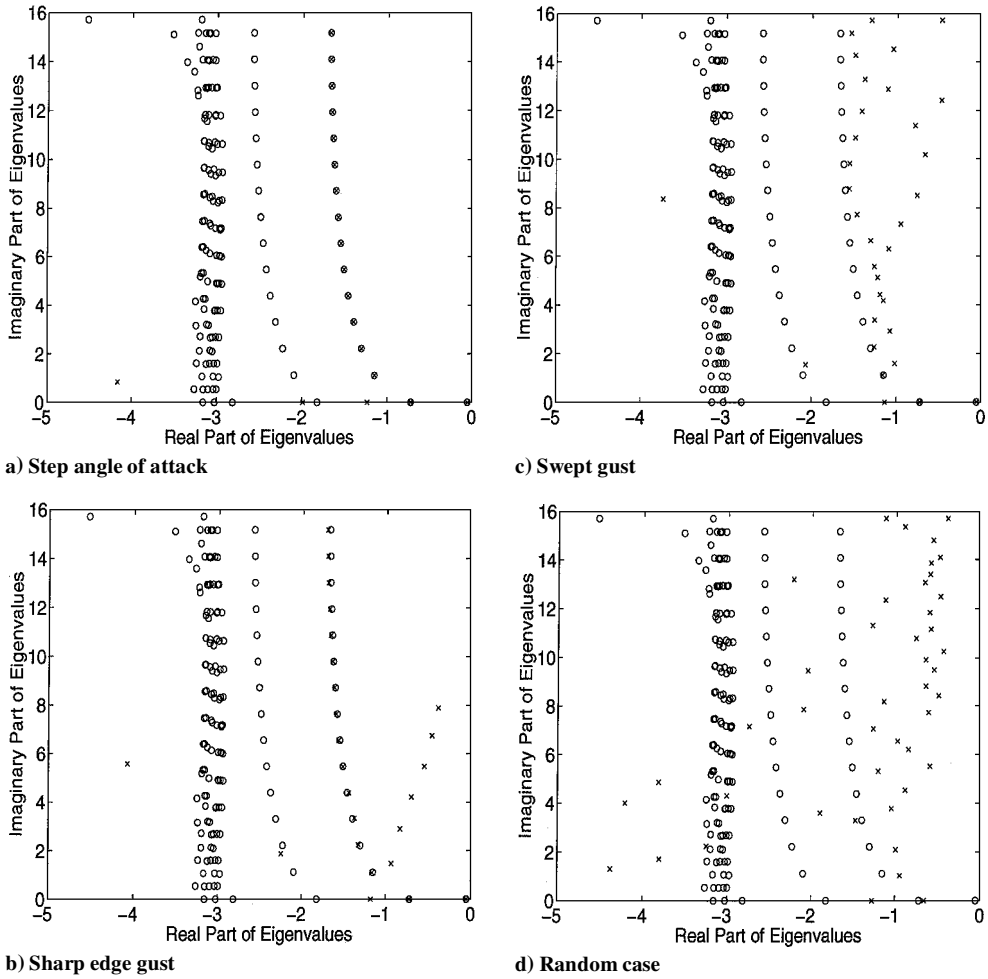

Fig. 5 Original eigenvalues from VL code (∘) and eigenvalues from system ID model obtained using vortex strength data on the wing and in the wake (×).

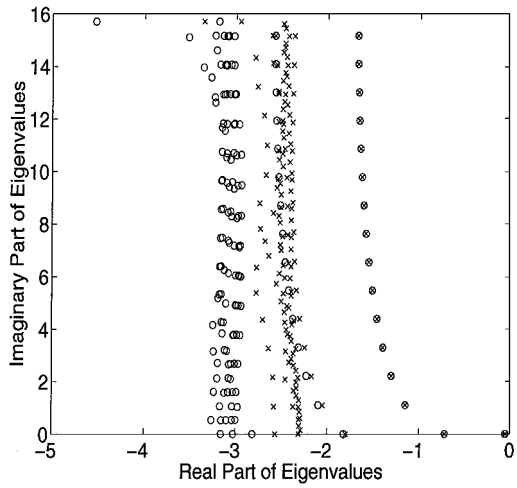

Fig. 6 Original eigenvalues from VL code (∘) and eigenvalues from system ID model obtained using vortex strength data on the wing and in the wake (×) for the random case when time series length is increased 10 times to 1000 time steps.

used to obtain the eigenvalues. The former case is shown in Figs. 5 and 6 and the latter in Fig. 7. Here the original VL eigenvalues are shown as circles, and the eigenvalues obtained from the SID model are indicated by crosses. In the case of full information, the dominant eigenvalue branch for the case of a step angle of attack (Fig. 5a) and also a sharp edge gust (Fig. 5b) is captured nicely (36 singular values and 57 singular values were used, respectively, in the SID model). For the case of a swept gust (Fig. 5c) and random downwash (Fig. 5d), the SID model produced sets of eigenvalues that do not agree well with the original ones from the VL code (164 singular values and 99 singular values were used, respectively, in the SID model). However, for the problem of the random downwash, increasing the length of the time history that was used as input to the SID model code from 100 to 1000 steps led to a set of eigenvalues that is in very good agreement with the dominant branch as shown in Fig. 6 (250 singular values were used).

When the vortex strengths only on the wing were used for some initial selection of parameters in the SID model (see Fig. 7), interestingly the dominant branch of eigenvalues is recovered not only for the step angle of attack (Fig. 7a) and the sharp edge gust (Fig. 7b), but also for the case of the swept gust (Fig. 7c) and random downwash (Fig. 7d), even though in the last case the dominant branch identified by the SID model is somewhat "off target." By looking at Fig. 7, one might conclude that providing vortex strength information only on the wing in these cases is sufficient for finding the distinct dominant eigenvalue branch. However, one should not conclude that using vortex strength information on the wing only is actually better than using information about vortex strengths both on the the wing and in the wake.

By running the SID code for various parameter choices and for a certain number of retained singular values, different lengths of time series, using information on the wing only vs information everywhere, etc., the authors have found, first, that the set of eigenvalues from the SID model could either include the "correct" dominant eigenvalue branch or could be a different set of eignvalues (which, by the way, does not prevent the SID model from reproducing the original time series with excellent agreement); second, it was concluded that if there is a distinct branch of eigenvalues found from the SID model it is most likely to be similar to the dominant branch in the original VL model.

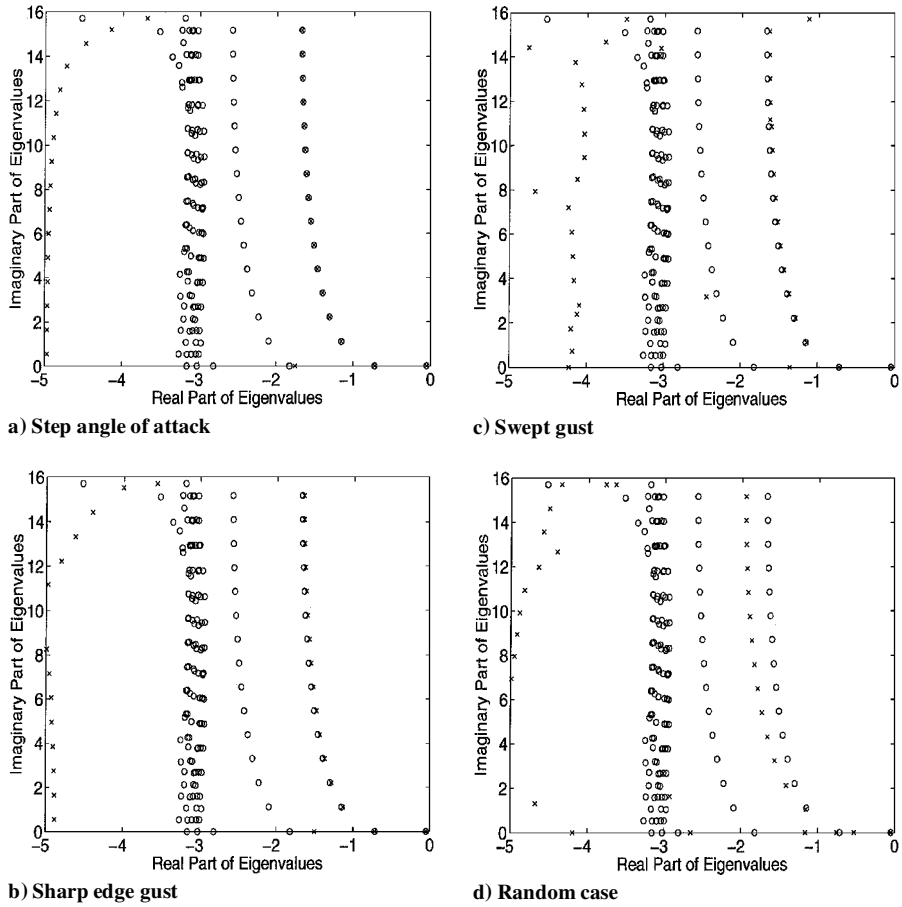

a) Step angle of attack

c) Swept gust

b) Sharp edge gust

d) Random case

Fig. 7 Original eigenvalues from VL code (∘) and eigenvalues from system ID model obtained using vortex strength data on the wing only (×).

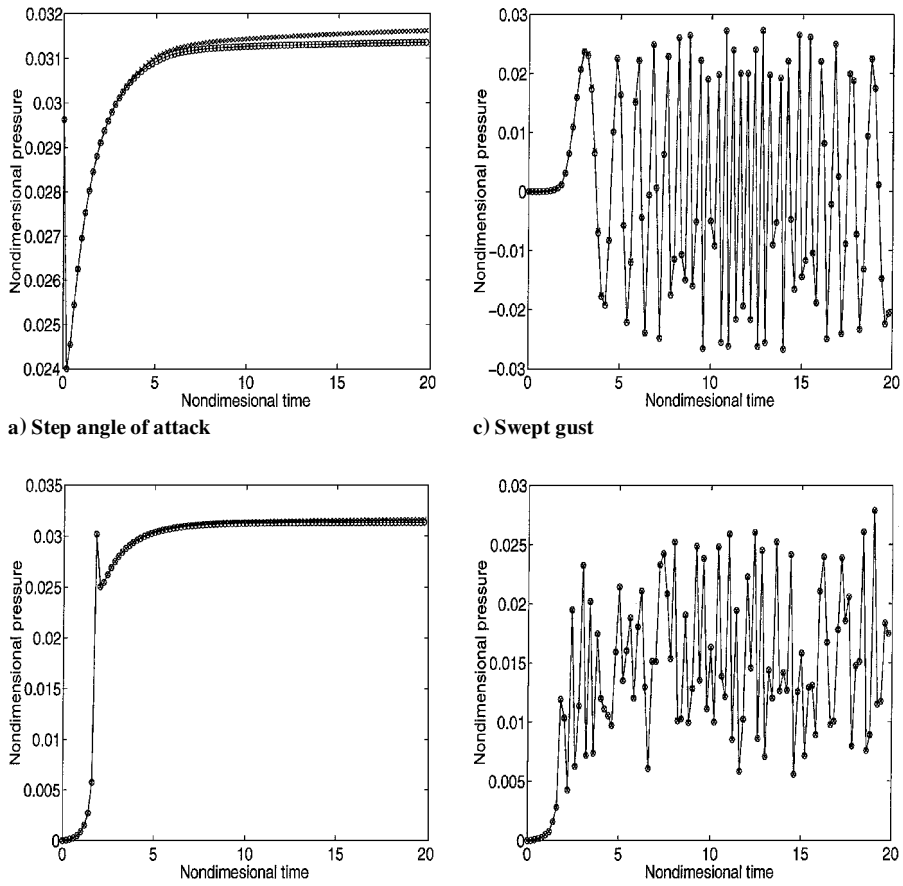

a) Step angle of attack

c) Swept gust

b) Sharp edge gust

d) Random case

Fig. 8 Time series of the pressure at the tip element. Original VL code data (—— with ∘) and the corresponding time series from the system ID model that was obtained using pressure on only 10 leading-edge elements as input (· · · · · with ×) for various flow excitations.

Now another case will be considered. In the context of wind-tunnel or flight experiments, one is also interested in what can be identified from measured data such as pressure. So using numerically simulated pressure values on the wing, the SID model was used to reproduce pressure time histories. Just as in the case of vortex strength data on the wing only, 55 pressure time histories of 100 time steps were input to the SID code. Using 30 to 40 singular values, the error between the original and identified time histories of pressure remained less than 1%.

One could argue that it may be impractical to use such a large number of sensors (55) on the wing to apply SID models. Thus, next only a portion of the pressure data on the wing was used. Different sensor positions were considered. A discussion of the various downwash and sensor locations on such a wing is ommitted here. For the current discussion leading-edge elements from the root to the tip of the wing were taken, as they appear to be a very good choice for system identification purposes. In Fig. 8 results for the pressure time history at the tip element of the wing are shown for the case when 10 measurements (still numerically simulated, of course) of the downwash and pressure time history (100 time steps) along the leading edge were supplied to create the SID model. Using from 50 to 90 singular values for the four aerodynamic loading problems, the already defined error ranged from 0.002 to 1.8%.

However, no success has yet been realized in approximating the eigenvalues of the original VL model using pressure data only. This is a subject of continuing investigation.

Conclusions

It has been shown that a modal representation of the aerodynamic forces acting on an oscillating wing has several attractive features that may be exploited. Starting from a numerical model of the fluid, here taken to be a vortex lattice model, the fluid model can be efficiently represented in terms of, for example, proper orthogonal decomposition (POD) modes. However it was also shown that using standard system identification techniques for linear dynamical systems, an identified system model can be constructed using data from the numerical model. Both the POD modes and the system identification method lead to substantially reduced-order models of the flowfield of comparable dimensions. Therefore, both provide highly efficient computational models relative to the original (vortex lattice) numerical model.

In principle the POD method can also be used for nonlinear dynamical systems. However, much work has yet to be done to implement this capability in the context of unsteady aerodynamic models. The system identification methodology for nonlinear dynamical systems is still a research frontier, and no general methods are yet available. On the other hand, the systems identification approach may be useful when only partial flowfield data are available, e.g., from a wind-tunnel experiment.

Finally it is noted that although a particular numerical model of the fluid was used in the present paper, i.e., a vortex lattice model, no special difficulty is expected in extending these methods to other computational fluid dynamics (CFD) models. Indeed the beneficial use of POD for a variety of CFD models has been shown in Refs. 1–3. Because the system identification model only requires time histories or Fourier series (frequency domain) data from such a CFD model, the extension to any time-linearized CFD model is straightforward. Indeed even if the original CFD model is not time linearized per se, the CFD code can be run for small wing motions to simulate numerically time linearized conditions.

Acknowledgments

This work was supported under the U.S. Air Force Office of Scientific Research Grant "Limit Cycle Oscillations and Nonlinear Aeroelastic Wing Response." Daniel Segalman is the Grant Program Officer. All numerical calculations were done on a supercomputer T916 in the North Carolina Supercomputing Center.

References

[1] Hall, K. C., "Eigenanalysis of Unsteady Flows About Airfoils, Cascades, and Wings," *AIAA Journal*, Vol. 32, No. 12, 1994, pp. 2426–2432.

[2] Dowell, E. H., Hall, K. C., and Romanowski, M. C., "Eigenmode Analysis in Unsteady Aerodynamics: Reduced Order Models," *Applied Mechanics Reviews*, Vol. 50, No. 6, 1997, pp. 371–385.

[3] Dowell, E. H., and Hall, K. C., "Modeling of Fluid-Structure Interaction," *Annual Review of Fluid Mechanics*, Vol. 33, 2001, pp. 445–490.

[4] Kim, T., "Frequency-Domain Karhunen-Loeve Method and Its Application to Linear Dynamic System," *AIAA Journal*, Vol. 36, No. 11, 1999, pp. 2117–2123.

[5] Juang, J.-N., *Applied System Identification*, Prentice–Hall, Upper Saddle River, NJ, 1994, Chap. 5.

A. Berman
Associate Editor